Islamic Azad University
Mashhad Branch

Ahmadzadeh and Zamani / Iranian Journal of Earth Sciences 8 (2016) / 25-35

A study of different zoning types in clinopyroxenes of sodic and potassic alkaline volcanic rocks from North Lahrud, NW Iran

Gholamreza Ahmadzadeh[*1], Reza Zamani[2]

1. Department of Geology, university of Mohaghegh Ardabili, Ardabil, Iran
2. Department of Geology, Meshginshahr Branch, Islamic Azad University, Meshginshahr, Iran

Received 10 May 2015; accepted 21 November 2016

Abstract

Clinopyroxene phenocrysts and microphenocrysts in potassic and sodic Eosen alkaline volcanic rocks from the northern Lahrud (NW Iran) record various stages in the crystallization and evolution history of the alkaline melt as well as its origin. The rock series hosting the clinopyroxene phenocrysts is phonolitic tephrite and tephritic phonolite composition. Theses rocks generally show porphyritic texture and have a variable phenocryst-rich nature (25–50%), with phenocryst assemblages characterized by Cpx ± An ± Pl. The studied clinopyroxenes have relatively high Mg-numbers (0.66-0.90), variable Al_2O_3 (3.77-7.31 wt%), low TiO_2 (<2.02 wt%) and Na_2O (<1.23 wt%) contents and low Al^{VI}/Al^{IV} ratios (mostly <0.25), suggesting relatively low-pressure crystallizing conditions of the magma in the magma chamber. The calculated pressures for the clinopyroxenes in these rocks vary in the range of 4–5.5 kbars. Oscillatory reverse zoning of clinopyroxenes related to the different crystallization paths under a variable oxygen fugacity and different oxidation conditions and sudden pressure differentiation and magma mixing processes. Normal zoning related to the differentiation and fractional crystallization of the magma. The resorption texture of core parts of some clinopyroxenes are attributed to the changes of crystallization pressure though such textures have been ascribed to magma mixing.

Keywords: *alkaline volcanic, clinopyroxene, sodic and potassic, magma mixing, NW Iran*

1. Introduction

Ca-rich clinopyroxene is one of the most common ferromagnesian minerals in alkaline potassic and sodic rocks from various tectonic settings, and has been used as a petrogenetic indicator for distinct magmatic series. But the occurrence of Ca-rich clinopyroxene phenocrysts in alkaline volcanic rocks from collision zone or post-collision setting is generally rare and has been considered to provide important clues to the nature of crystallization and evolution of related magmas. Crystal chemical studies on clinopyroxenes have provided useful information about the origin of parental magmas and petrological evolution of host rocks (e.g., (Bindi et al. 1999; Avanzinelli et al. 2004)). Several studies have shown that compositional variations in the clinopyroxenes can be used as petrogenetic indicators (Dal Negro et al. 1982; Dal Negro et al. 1986; Manoli and Molin 1988; Bizimis et al. 2000; Ghorbani and Middlemost 2000; Princivalle et al. 2000; Nazzareni et al. 2001; Avanzinelli et al. 2004; Zhu and Ogasawara 2004). In particular, most of the clinopyroxenes in alkaline rocks show different types of zoning such as oscillatory, sectoral, and complex.

---

*Corresponding author.
E-mail address (es): gholamrezaahmadzadeh@yahoo.com

Oscillatory zoning may generally indicate cyclic changes in crystallization conditions (Federico et al. 1988; Shimizu 1990) or different crystallization paths under variable fluid regime (Sazonova and Nosova 1999). On the other hand, the origin of complex and reversed zoning clinopyroxene phenocrysts with resorption is ascribed to magma mixing by many researches (e.g., (Wass 1979; Duda and Schmincke 1985; Dobosi and Fodor 1992; Simonetti et al. 1996; Aldanmaz 2006), and this is generally called a co-magmatic origin (Vollmer et al. 1981; Barton et al. 1982). In some cases, the clinopyroxenes that are not genetically related to the host lavas are interpreted to have crystallized at high pressures from magmas, and these clinopyroxenes are called xenocrystic origin (Shaw and Eyzaguirre 2000). Crystallization pressure of the clinopyroxenes in magmatic systems has also been investigated by several authors. Dal Negro et al. (1989) qualitatively discussed the influence of crystallization pressure of on the crystal-chemistry of the clinopyroxenes, and Malgarotto et al. (1993) also estimated the crystallization pressures of their samples with the clinopyroxenes. More recently, an efficient clinopyroxene geobarometer was proposed by Nimis (1995); Nimis and Ulmer (1998); Nimis (1999), thus providing an opportunity to constrain the depths of magma chambers in the crustal levels.

2. Geological setting

The study area is situated in the northern Lahrud, NW Iran (Fig. 1). Based on the classification of Iran's structural units, this area is part of the Eocene-age, E-W trending Alborz-Azerbaijan magmatic belt that is related to the western division of the Alborz Cenozoic volcanic belt. The Alborz Cenozoic volcanic belt is divided into western and eastern parts by the N-S trending Rasht-Takestan Fault (Azizi and Moinevaziri 2009). This volcanic belt is separated from the central Iranian plate to the south by the Tabriz Fault and to the north, and extends into Armenia (Azizi and Jahangiri 2008a). Volcanic and plutonic rocks of Eocene and Plio-Quaternary age are widely distributed in this Alborz-Azerbaijan-Lesser Caucasus magmatic belt and mainly comprise calc-alkaline to alkaline felsic to mafic volcanic rocks and felsic to intermediate intrusions (Moayyed 2001; Jamali et al. 2012). Almost coincidental with the closing of the Neo-Tethys ocean in the Zagros Belt and related branches around central Iran, the Sevan-Akera-Qaradagh Ocean (or northern branches of the Neo-Tethys) was closed in north-central Iran (Azerbaijan) in the late Cretaceous (Aghanabati 2004). The magmatism in the Alborz-Azerbaijan belt is probably related to the closure of this basin. The study area comprises alkaline lavas and pyroclastic rocks associated with sedimentary and volcano-sedimentary units (Fig. 2). In addition, a number of small sub-volcanic bodies of the Oligocene age are exposed in the south-western part of the area. Phonotephrite and trachyandesite feeder dykes of the volcanic units locally cut volcanic breccias and form parallel sets. The volcanic rocks include analcime-bearing and analcime-free lavas locally associated with volcanic breccias and pillow lava. Submarine lava eruptions formed widespread volcanic breccias, pillow lavas, and clastic rocks in the early Eocene.

3. Petrography

Based on mineral assemblages mafic alkaline rocks is exposed over a wide area and is characterized by feldspar (plagioclase and alkaline feldspar; estimated vol. 25–40% and 10–30% respectively), clinopyroxene (15–40%) and analcime (10–30%) phenocrysts set in a microlithic groundmass of feldspar with minor clinopyroxene, analcime and volcanic glass. Most samples show porphyritic texture with vitrophyric textures in the groundmass. Oscillatory zoning is also observed in plagioclase. More evolved rocks contain sanidine with rare Carlsbad twinning as phenocryst and groundmass mineral. Clinopyroxene phenocrysts, 1–6 mm long, are found in all rock types and often show both oscillatory and sector zoning (Fig. 3a). Locally, clinopyroxene shows glomeroporphyritic textures. Melt inclusions in some clinopyroxenes possibly indicate crystallization under disequilibrium conditions (Fig. 3b). Some clinopyroxenes show oscillatory normal and reverse type of zoning (Fig 3a–d). Trapezohedral analcime phenocrysts are up to 2 cm in size and commonly show radial cracks. Apatite and opaque minerals occur as accessory minerals in the groundmass, and apatite also forms inclusions in clinopyroxene phenocrysts.

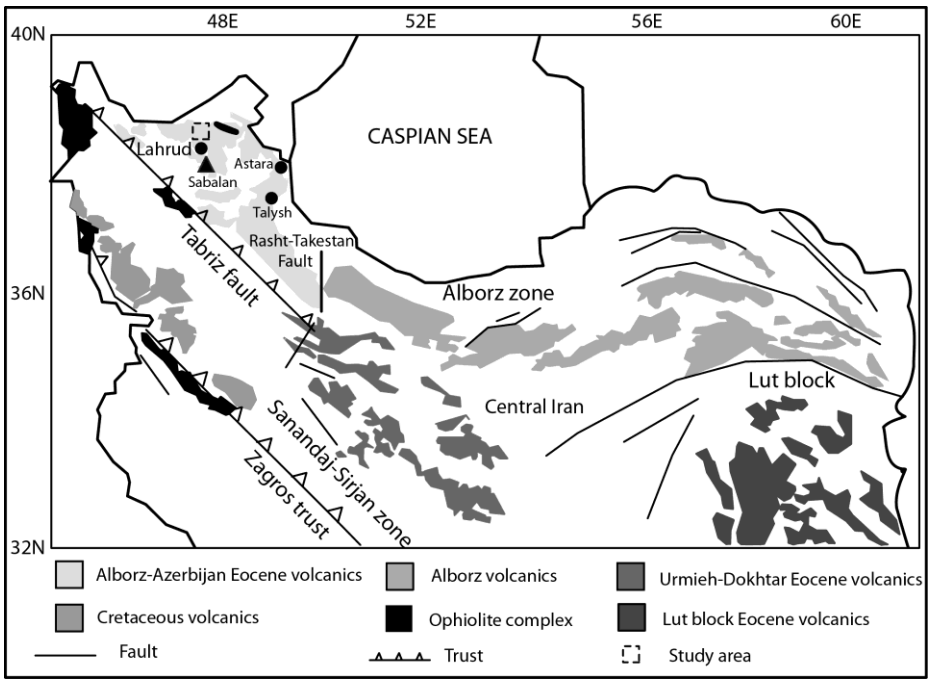

Fig. 1. Distribution of Cretaceous and Eocene volcanic rocks and dismembered ophiolites in Iran (after Azizi and Jahangiri (2008b)).

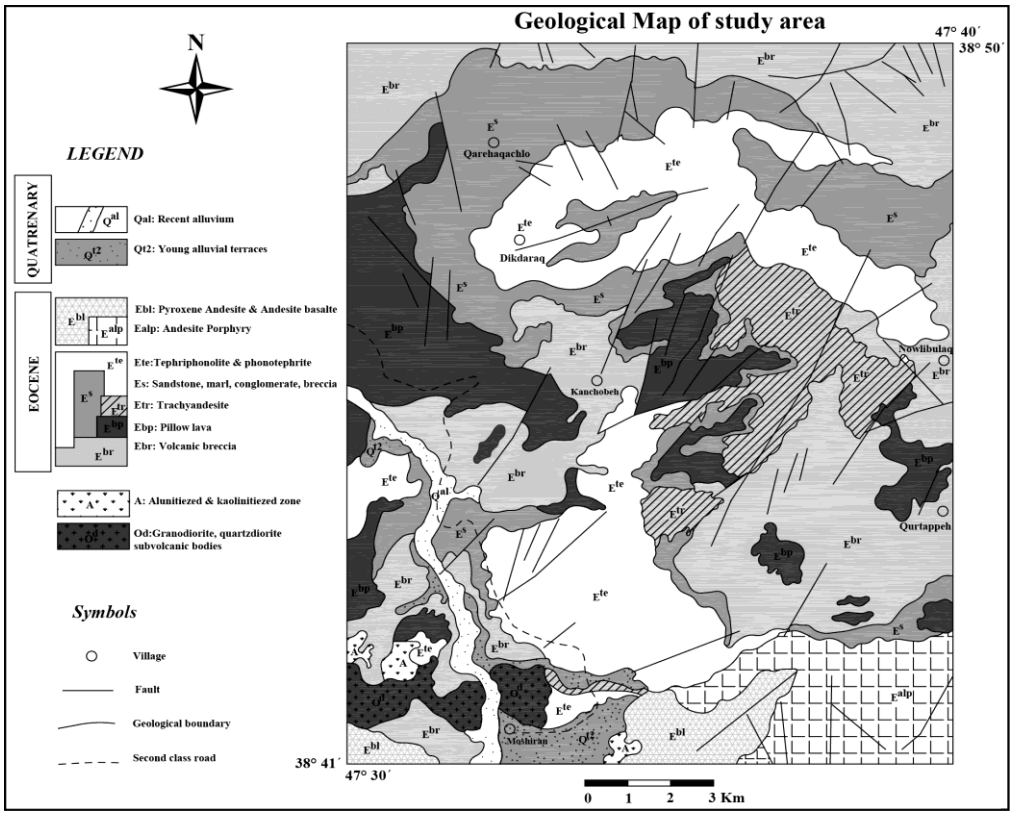

Fig. 2. Modified geological map of the study area (NE Meshginshahr).

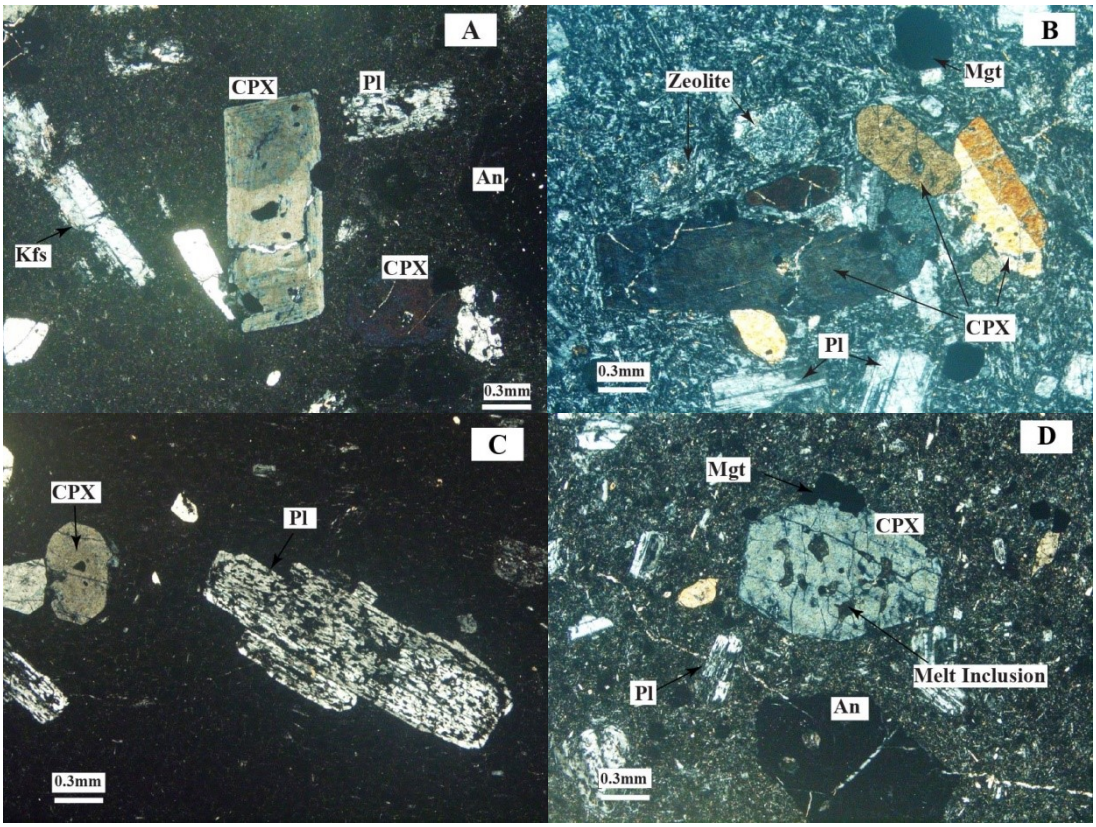

Fig. 3. Microscopic from sodic and potassic alkaline rocks show different zoning type of clinopyroxenes.

4. Analytical Methods

Polished thin sections of the clinopyroxenes were studied in detail by using optical methods before microprobe analyses. For determination of the major element composition, a number of euhedral and subhedral clinopyroxenes were analyzed. Chemical analyses of the clinopyroxenes were performed by using a CAMECA-SX-100 electron microprobe at the mineralogical lab of Manitoba University, Canada.

5. Clinopyroxene composition and classification

Major representative element compositions and site occupancies of the investigated clinopyroxenes are presented in Table 1. The crystals have generally high Mg numbers [Mg/(Mg+Fe^{2+})] of 0.66–0.90, variable Al_2O_3 (3.77–7.21 wt%), low TiO_2 (<2.02 wt%) and Na_2O (<1.23 wt%) contents and low $Al^{[6]}/Al^{[4]}$ ratios (generally <0.5). In the conventional classification diagram (Morimoto et al., 1988) all clinopyroxenes are salite in composition (Fig. 4a, b). In the Ti–Na- $Al^{[4]}$ triangular diagram of Papike et al. (1974), the compositions of most of clinopyroxenes fall in the Ca-Tschermark's molecule (CATS) field (Fig. 5). The moderate to high Al/Ti (5.2–12.6) and low Al^{VI}/Al^{IV} (mostly <0.25) ratios typically reflect low pressure igneous clinopyroxenes (Aoki and Shiba 1973). The low Na contents indicates that the clinopyroxenes in the area rocks are poor in acmite.

Clinopyroxenes of mafic alkaline series display high content of Al^{3+} and are present mostly on the Tsite and to a lesser extent on the M1 site, as in clinopyroxenes from potassic alkaline volcanic province in Italy (Bindi et al. 1999; Avanzinelli et al. 2004). The M1 site is dominated by Mg (0.507–0.690 a.f.u.) with minor amounts of Fe^{2+} (0.101–0.235 a.f.u.) and R^{3+} ($Al^{VI}+Fe^{3+}+Cr^{3+}+Ti^{4+}$ = 0.20 - 0.28 a.f.u.). The M2 site is almost fully occupied by Ca (0.872 - 0.913 a.f.u.), while Na (<0.113 a.f.u.), Mn (<0.037 a.f.u.) and Mg M2 (0.002–0.033 a.f.u.) are characteristically low (Table 1). In all clinopyroxenes, Al T is sufficient to completely fill the deficiency of Si^{4+} in the tetrahedral sites. The observed differences in the Fe^{3+} content can be explained by different oxidation states or diverse oxygen fugacity of the magmas (Canil and Fedortchouk 2000; Aydin et al. 2008), although the use of the Al^{VI}+2Ti+Cr versus Al^{IV}+Na diagram (Bence et al. 1975) shows that all the samples fall on the upper side of the Fe^{3+} line, indicating a high oxygen fugacity of the magma (Fig. 6).

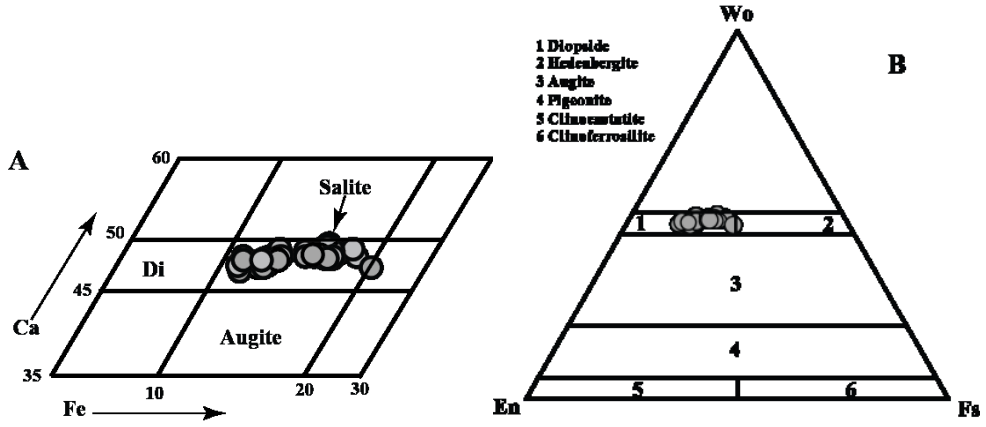

Fig.4- conventional classification diagram (Morimoto et al. 1988), all clinopyroxenes are salite in composition.

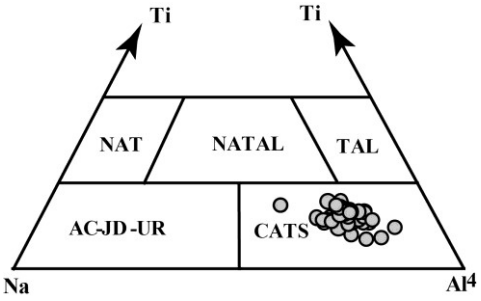

Fig. 5. The Ti–Na- $Al^{[4]}$ triangular diagram of (Papike et al. 1974), the compositions of most of clinopyroxenes fall in the Ca-Tschermark's molecule (CATS) field.

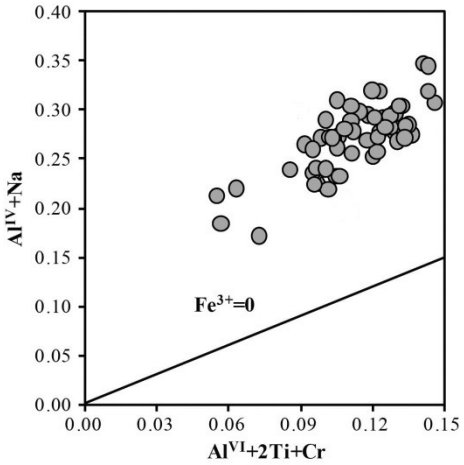

Fig. 6. The Al^{VI}+2Ti+Cr versus Al^{IV}+Na diagram (Bence et al. 1975) shows all the samples fall in the upper side of Fe^{3+} line.

6. Clinopyroxene zoning

Representative chemical data for zoning types in the clinopyroxenes are given in Table 1. Analysis has been done along a core to rim profile of clinopyroxene phenocrysts. We recognized the following types of zoning: i) zoning related to the crystallization of melt (oscillatory and sectoral zoning), ii) zoning related to different crystallization paths under a variable fluid regime (oscillatory, reverse zoning), iii) zoning related to fractionation of crystallizing magma (normal zoning, i.e., enrichment of Fe, Al and Ti in at rims). The zoning types will be presented in detail below.

I) Oscillatory, reverse zoning is occasionally observed in the clinopyroxenes of the studied samples (Fig. 7). In particular, these clinopyroxenes consist of three distinct regions: core, intermediate zone, and rim. The core has a nearly homogenous composition, characterized by lower Mg content and higher Fe, Al, and Ti concentrations. In the intermediate zone, the trends are reversed (i.e., reversed zoning): Mg gradually increases, whereas Fe, Al, and Ti relatively decrease towards rims. The third compositional region along the profiles displays a very thin clinopyroxene rim that has a nearly homogenous composition in terms of all the elements. The three stages, in our opinion, show a change from the constant to different crystallization paths and probably reflect the following three stages in the crystallization of the melt: (1) relatively low-pressure crystallization under a constant fluid regime, (2) different crystallization paths under a variable fluid regime, (3) variable oxygen fugacity and different oxidation condition and sudden pressure differentiation, (4) magma mixing.

II) Normal zoning is usually observed in the clinopyroxenes of the mafic alkaline rocks as can be seen in (Fig. 8). This phenocryst shows generally normal zoning with enrichment of Fe^{2+}, Al, and Ti from core to rim compared to those of the other clinopyroxenes, which is the direct result of magmatic fractionation. However, it consists of three distinct regions: core, mantle, and rim. The core has a nearly homogenous composition. It is characterized by higher Mg and Ca concentrations and lower Fe, Al, and Ti contents (Fig. 8). This character of crystallization is most common in relatively deep-seated quiet environments (<15 km) devoid of sudden changes in the intensive parameters of the magmatic system. The mantle is made up of strong oscillation zones, making it possible to clearly distinguish the oscillatory zoning from the core. The oscillatory zoning shows an overall increasing trend for Fe, Al, and Ti, and a decreasing concentration trend for Mg and Ca throughout the mantle. Finally, the rim has a nearly homogenous composition, with relatively decreasing Mg and Ca. Hence, these characters point to a normal process of melt fractionation and the variations in the crystallization conditions of the clinopyroxens.

7. Discussion

7.1. P-T Conditions of Clinopyroxenes

The investigated clinopyroxenes mostly fall in the 'igneous rocks' field of Aoki and Shiba (1973) according to the $Al^{[6]}$ vs. $Al^{[4]}$ diagram. Their Al^{VI}/Al^{IV} ratios are generally lower than 0.25, indicating a relatively low-pressure crystallization (Fig. 9a).They differ from those in xenoliths of mantle lherzolite (Dawson 1987) and high pressure clinopyroxenes (Simonetti et al. 1996) in having lower $Mg^{\#}$ (0.68–0.95, Fig. 9b) and very low Cr_2O_3 (0.0–0.2 wt%), Al_2O_3 (<9.6 wt%), Na_2O (<0.9 wt%) contents. A more quantitative estimation of pressure can be acquired with the equations proposed by Nimis (1995); Nimis (1999). In this study, we have calculated the pressure by using the Cpx-geobarometer proposed by Nimis (1999), which can be used for basic tholeiitic to alkaline magmas. The equilibrium temperatures were estimated by using the equation based on the experimental work of Putirka et al. (2003). The chemical variations between the core and rim compositions of the clinopyroxenes in these rocks do not affect significantly the estimated equilibrium pressures and intra-crystalline closure temperatures, leading to a range of 3-5.5 kbars and 950–1080^{oC} for the Cpx compositions.

Table 1. Representative microprobe analyses of clinopyroxene phenocrysts in volcanic rocks of study area.

	Core				Rim	Core					Rim
	1-1	1-2	1-3	1-4	1-5	2-1	2-2	2-3	2-4	2-5	2-6
SiO_2	49.79	46	48.11	47.74	48.65	47.26	47.23	48.65	48.36	48.07	49.03
TiO_2	0.95	1.19	1.16	1.15	1.04	1.44	1.53	1.13	1.18	1.22	0.98
Al_2O_3	4.39	7.92	5.02	5.68	4.96	6.16	6.14	4.86	5.51	5.67	4.63
FeO	7.94	9.02	8.25	8.73	8.34	8.71	8.8	8.06	8.5	8.63	8.47
Fe_2O_3	0.00	0.00	0.00	0.00	0.00	0.00	0.00	0.00	0.00	0.00	0.00
MnO	0.47	0.28	0.4	0.52	0.45	0.45	0.4	0.42	0.52	0.41	0.46
MgO	12.8	11.56	12.84	12.11	12.68	12.12	12.1	12.99	12.29	12.17	12.57
CaO	21.95	22.67	22.21	21.59	21.86	22.09	22.37	22.36	21.95	22.12	21.92
Na_2O	0.81	0.48	0.68	0.95	0.81	0.88	0.68	0.73	0.87	0.82	0.82
K_2O	0.00	0.00	0.00	0.00	0.00	0.00	0.00	0.00	0.00	0.00	0.00
Cr_2O_3	0.00	0.00	0.00	0.00	0.00	0.00	0.00	0.00	0.00	0.00	0.00
Total	99.1	99.12	98.67	98.47	98.79	99.11	99.25	99.2	99.18	99.11	98.88
Site T											
Si	1.863	1.728	1.809	1.800	1.827	1.772	1.772	1.818	1.811	1.803	1.841
Al^{IV}	0.137	0.272	0.191	0.200	0.173	0.228	0.228	0.182	0.189	0.197	0.159
Site M_1											
Al^{VI}	0.057	0.079	0.031	0.053	0.046	0.044	0.043	0.032	0.054	0.053	0.046
Fe(III)	0.085	0.160	0.144	0.151	0.127	0.167	0.148	0.140	0.132	0.135	0.117
Cr	0.000	0.000	0.000	0.000	0.000	0.000	0.000	0.000	0.000	0.000	0.000
Ti	0.027	0.034	0.033	0.033	0.029	0.041	0.043	0.032	0.033	0.034	0.028
Fe(II)	0.155	0.116	0.109	0.118	0.127	0.101	0.121	0.107	0.128	0.129	0.142
Mg	0.676	0.611	0.683	0.646	0.670	0.647	0.644	0.690	0.653	0.648	0.668
Site M_2											
Mg	0.038	0.037	0.037	0.035	0.040	0.030	0.033	0.034	0.033	0.032	0.036
Fe(II)	0.009	0.007	0.006	0.006	0.008	0.005	0.006	0.005	0.007	0.006	0.008
Mn	0.015	0.009	0.013	0.017	0.014	0.014	0.013	0.013	0.016	0.013	0.015
Ca	0.880	0.913	0.895	0.872	0.879	0.887	0.899	0.895	0.881	0.889	0.882
Na	0.059	0.035	0.050	0.069	0.059	0.064	0.049	0.053	0.063	0.060	0.060
K	0.000	0.000	0.000	0.000	0.000	0.000	0.000	0.000	0.000	0.000	0.000
Wo	47.4	49.3	47.4	47.3	47.1	47.9	48.2	47.5	47.6	48.0	47.3
En	38.4	35.0	38.2	36.9	38.1	36.6	36.3	38.4	37.1	36.7	37.7
Fs	14.2	15.8	14.4	15.8	14.8	15.5	15.5	14.1	15.3	15.3	15.0
Mg#	0.81	0.84	0.86	0.85	0.84	0.87	0.84	0.87	0.84	0.83	0.83
R^{3+}	0.17	0.27	0.21	0.24	0.20	0.25	0.23	0.20	0.22	0.22	0.19

Structural formulae calculated on the basis of six oxygen, Mg# = $(Mg/Mg+Fe^{2+})$, $R^{3+}= (Al^{vi}+Fe^{3+}+Cr^{3+}+Ti^{4+})$

Table 1. (continued)

	Core										Rim
	3-6	**3-7**	**3-8**	**3-9**	**3-10**	**3-11**	**3-12**	**3-13**	**3-14**	**3-15**	**3-16**
SiO_2	46.21	45.55	45.51	46.1	46.07	47.12	47.56	47.09	46.71	46.72	46.91
TiO_2	1.98	1.72	2.02	1.62	1.73	1.45	1.32	1.64	1.78	1.5	1.73
Al_2O_3	5.6	6.27	6.79	5.58	6.12	5.16	4.85	5.53	5.34	5.41	3.87
FeO	11.73	11.08	12.26	11.42	11.78	11.04	10.42	10.92	11.4	10.65	13.43
Fe_2O_3	0.00	0.00	0.00	0.00	0.00	0.00	0.00	0.00	0.00	0.00	0.00
MnO	0.74	0.75	0.76	0.72	0.77	0.71	0.72	0.81	0.82	0.72	1.14
MgO	9.9	10.09	8.94	10.02	9.98	10.49	10.97	10.31	10.14	10.63	8.7
CaO	21.82	22.25	21.81	22.29	22.13	22.38	22.31	22.15	21.9	22.26	20.9
Na_2O	0.94	0.82	1.09	0.95	0.91	0.82	0.85	0.91	0.96	0.81	1.5
K_2O	0.00	0.00	0.00	0.00	0.00	0.00	0.00	0.00	0.00	0.00	0.00
Cr_2O_3	0.00	0.00	0.00	0.00	0.00	0.00	0.00	0.00	0.00	0.00	0.00
Total	98.92	98.53	99.18	98.7	99.49	99.17	99	99.36	99.05	98.7	98.18
Site T											
Si	1.766	1.742	1.738	1.761	1.748	1.789	1.803	1.785	1.779	1.780	1.818
Al^{IV}	0.234	0.258	0.262	0.239	0.252	0.211	0.197	0.215	0.221	0.220	0.177
Site M_1											
Al^{VI}	0.018	0.024	0.044	0.012	0.021	0.020	0.020	0.032	0.019	0.023	0.000
Fe(III)	0.173	0.196	0.183	0.204	0.199	0.168	0.164	0.156	0.171	0.172	0.200
Cr	0.000	0.000	0.000	0.000	0.000	0.000	0.000	0.000	0.000	0.000	0.000
Ti	0.057	0.049	0.058	0.047	0.049	0.041	0.038	0.047	0.051	0.043	0.050
Fe(II)	0.199	0.158	0.208	0.161	0.173	0.181	0.165	0.188	0.190	0.166	0.235
Mg	0.554	0.573	0.507	0.575	0.558	0.589	0.614	0.577	0.569	0.597	0.515
Site M_2											
Mg	0.010	0.003	0.002	0.00	0.007	0.005	0.006	0.006	0.007	0.007	-0.01
Fe(II)	0.004	0.001	0.001	0.000	0.002	0.001	0.002	0.002	0.002	0.002	0.000
Mn	0.024	0.024	0.025	0.023	0.025	0.023	0.023	0.026	0.026	0.023	0.037
Ca	0.893	0.912	0.892	0.912	0.899	0.911	0.906	0.900	0.894	0.908	0.868
Na	0.070	0.061	0.081	0.070	0.067	0.060	0.062	0.067	0.071	0.060	0.113
K	0.000	0.000	0.000	0.000	0.000	0.000	0.000	0.000	0.000	0.000	0.000
Wo	48.1	48.9	49.1	48.8	48.3	48.5	48.2	48.5	48.1	48.5	47.1
En	30.4	30.8	28.0	30.5	30.3	31.6	33.0	31.4	31.0	32.2	27.3
Fs	21.5	20.3	22.9	20.7	21.4	19.9	18.8	20.1	21.0	19.3	25.6
Mg#	0.74	0.78	0.71	0.78	0.76	0.76	0.79	0.75	0.75	0.78	0.68
R^{3+}	0.25	0.27	0.28	0.26	0.27	0.23	0.22	0.24	0.24	0.24	0.25

Structural formulae calculated on the basis of six oxygen, $Mg\# = (Mg/Mg+Fe^{2+}), R^{3+} = (Al^{VI}+Fe^{3+}+Cr^{3+}+Ti^{4+})$

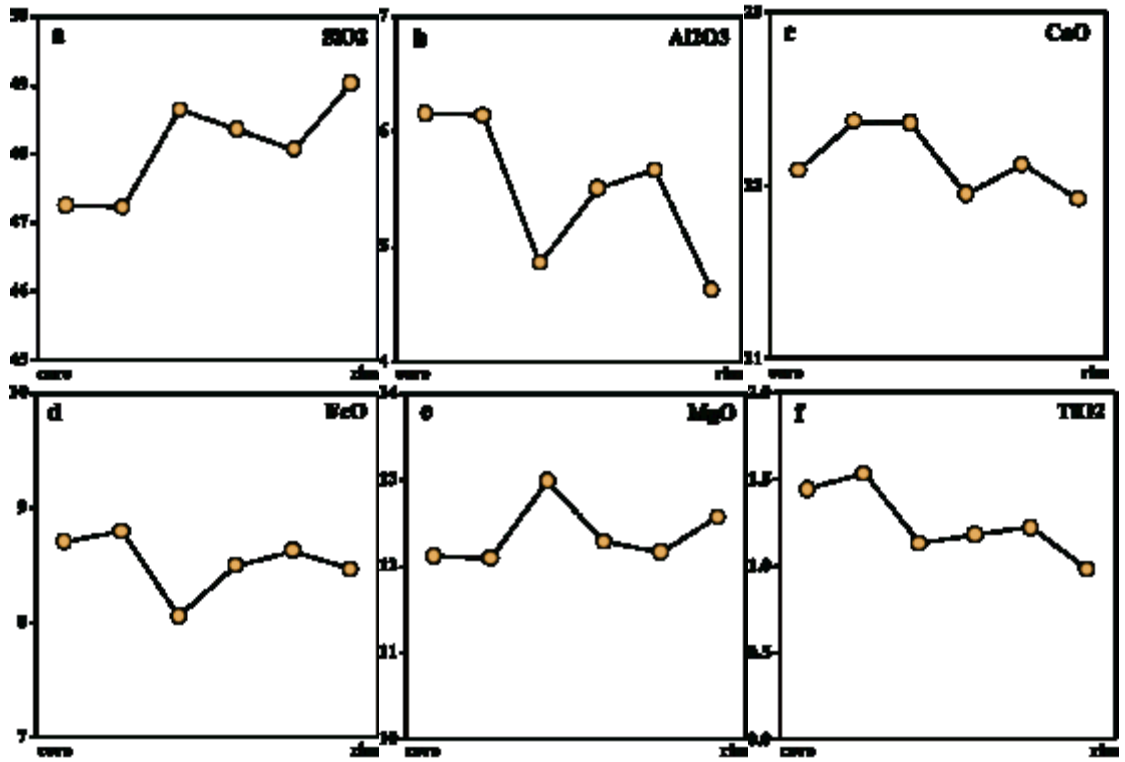

Fig. 7. Oscillatory, reverse zoning is occasionally observed in the clinopyroxenes of studied samples.

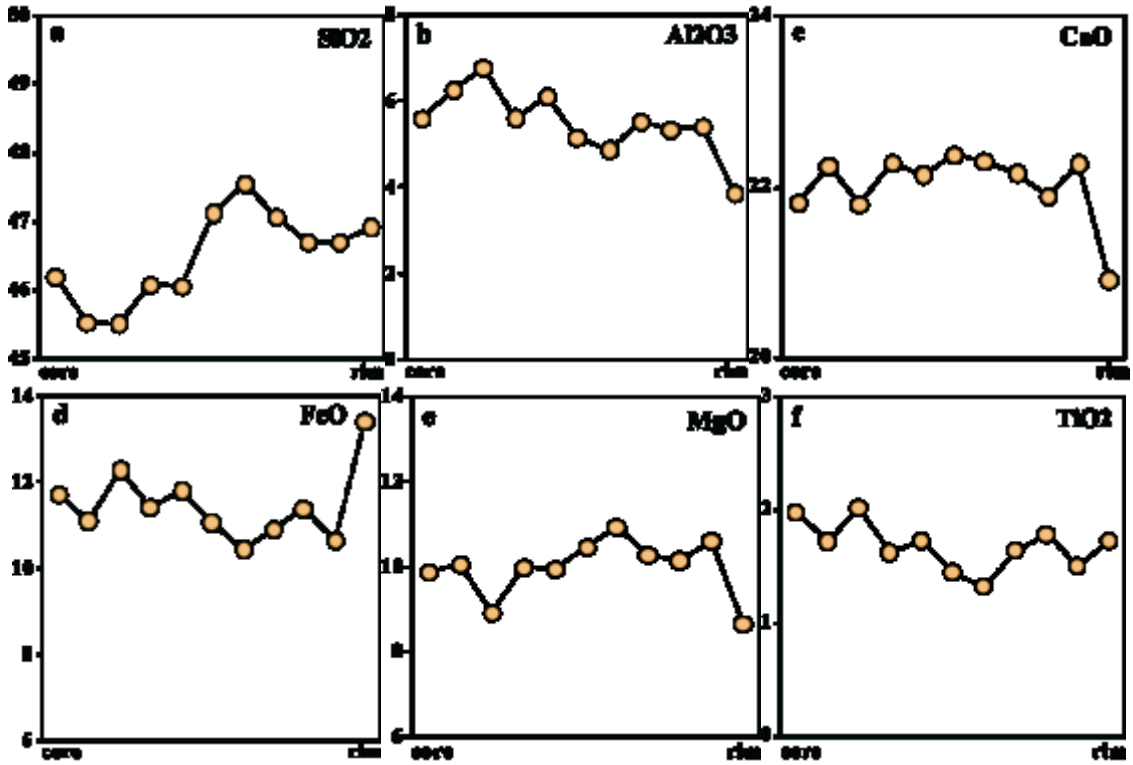

Fig. 8. Normal zoning is usually observed in the clinopyroxenes of the mafic alkaline rocks.

According to the Mg number versus Na diagram (Fig. 9b), it can be said that there are little differences between the estimated pressures from the Na-Mg$^{\#}$ variation diagram and those from calculations. According to this diagram, most of the samples show pressure in the range of 5–10 kb. However, the quantitative results, mostly based on Ti, Cr and Al[6] contents, are lower than 10 kbars. As a result, it can be

said that the studied clinopyroxenes do not have sufficient Na content compared to the clinopyroxene phenocrysts from different locations, and thus do not resemble the high-pressure (>15 kbars) ones. However, the different pressures values in these clinopyroxenes are related to the crystallization of clinopyroxenes at different levels and depths of magma chamber station in the ascent path of magma from the lower mantel to the crust.

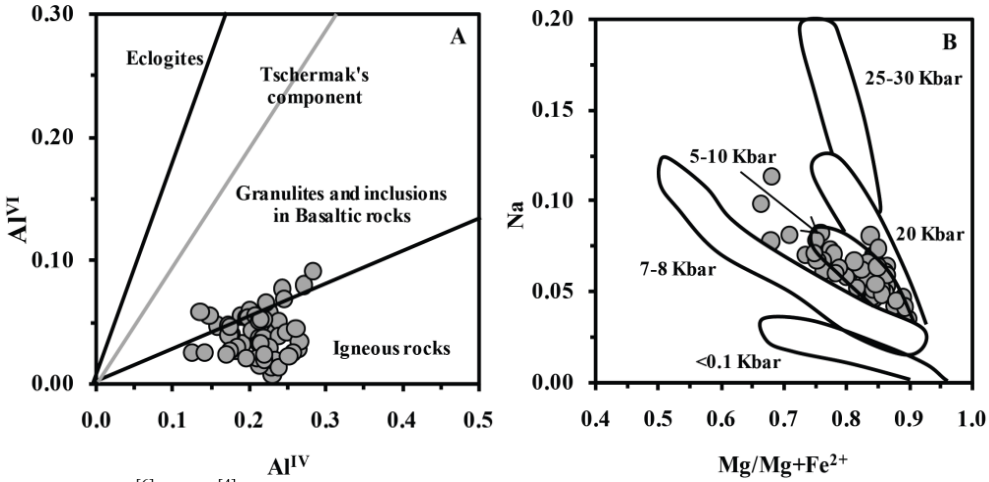

Fig. 9. a) According to the $Al^{[6]}$ vs. $Al^{[4]}$ diagram, the investigated clinopyroxenes mostly fall in the 'igneous rocks' field of Canil and Fedortchouk (2000). b) Mg number versus Na diagram (Simonetti et al. 1996).

7.2. Causes of Zoning Types in Clinopyroxenes

Various hypotheses can be considered to explain the occurrence of different zoning types in the studied clinopyroxenes.

1. A possible hypothesis is that the core and rim and mantle band compositions of the clinopyroxenes crystallized at different pressures (Wass 1979; Dobosi and Horváth 1988). Figures 8 and 9 show different diagrams for cores and rims of the clinopyroxenes, and for groundmass crystals. These diagrams provide us useful information on the crystallization pressure of the clinopyroxenes, showing no considerable difference between the crystallization pressures of the cores and rims of the studied clinopyroxenes.

2. The mixing process has been recognized as one of the main process that can induce disequilibrium phenomena such as complex or reverse zoning and resorption/reaction textures. Indeed, most of the disequilibrium textures are ascribed to magma mixing by many researches (Wass 1979; Duda and Schmincke 1985; Dobosi and Fodor 1992; Simonetti et al. 1996). Such a process is known to have the ability to generate strong heterogeneities within magma bodies on very short scales (Perugini et al. 2002; Perugini et al. 2003). The presence of colourless diopside cores with sharply contrasting green salite rims is the best evidence in support of magma mixing. The sharp compositional differences between diopside cores and salite rims suggest that the cores and rims crystallized from two melts with different chemical composition. Dissolution of clinopyroxenes cores, which led to the formation of strongly resorbed margins and a network of internal cavities within the Cpx, indicate disequilibrium between cores of Cpx and melt. The presence of Mg- and Cr-rich bands and resorbed texture in some clinopyroxenes of potassic and sodic volcanic rocks of Lahrud, indicate that magma mixing of primary magma with some differentiated magma can be reason for such texture and zonings.

3. Considering the effect of oxygen fugacity, the Fe3+/Fe ratio for the clinopyroxenes (mean=0.14) is significantly lower. This is interpreted here to be evidence of different oxidation states for the formation of the core and rim. Although changes in the Fe^{3+}/Fe ratio of the clinopyroxenes occur between the core and the rim, it is less significant among different zones of the salite rim. Therefore, the complex zoning of the rim cannot be explained by the oxidation state of the magma, as discussed by Hamilton et al. (1964); Brooks and Rucklidge (1973). They suggested that the changes in oxygen fugacity due to, for example; the release of volatile or contamination might explain the rapid changes in clinopyroxene compositions toward the Fe^{3+}- rich type. Oxygen fugacity may have risen as a result of contamination (Hamilton et al. 1964) and could have a genetic link with the green rim.

8. Conclusion

Mineral chemistry studies show clinopyroxenes of the study area with salite composition have relatively low-pressure crystallization conditions of the magma in the magma chamber. The calculated pressures for the clinopyroxenes in these rocks are in the range of 4–5.5 kbars. The analyses of the compositional trends of the clinopyroxenes indicate the oscillatory reverse zoning

in clinopyroxenes related to the different crystallization paths under a variable oxygen fugacity and different oxidation condition and magma mixing processes. Normal zoning is related to the differentiation and fractional crystallization of the magma. The resorption texture of core parts of some clinopyroxenes are attributed to the changes of crystallization pressure, though such textures have been ascribed to magma mixing. Crystallized clinopyroxenes underwent a relatively low-pressure fractional crystallization process in closed-magma chambers at different levels of the crust.

References:

Aghanabati A (2004) Geology of Iran. Geological survey of Iran.

Aldanmaz E (2006) Mineral-chemical constraints on the Miocene calc-alkaline and shoshonitic volcanic rocks of western Turkey: disequilibrium phenocryst assemblages as indicators of magma storage and mixing conditions, *Turkish Journal of Earth Sciences* 15:47-73.

Aoki K-I, Shiba I (1973) Pyroxenes from lherzolite inclusions of Itinome-gata, Japan, *Lithos* 6:41-51.

Avanzinelli R, Bindi L, Menchetti S, Conticelli S (2004) Crystallisation and genesis of peralkaline magmas from Pantelleria Volcano, Italy: an integrated petrological and crystal-chemical study, *Lithos* 73:41-69.

Aydin F, Karsli O, Chen B (2008) Petrogenesis of the Neogene alkaline volcanics with implications for post-collisional lithospheric thinning of the Eastern Pontides, NE Turkey, *Lithos* 104:249-266.

Azizi H, Jahangiri A (2008a) Cretaceous subduction-related volcanism in the northern Sanandaj-Sirjan Zone, Iran, *Journal of Geodynamics* 45:178-190

Azizi H, Jahangiri A (2008b) Cretaceous subduction-related volcanism in the northern Sanandaj-Sirjan Zone, Iran, *Journal of Geodynamics* 45:178-190 doi:10.1016/j.jog.2007.11.001.

Azizi H, Moinevaziri H (2009) Review of the tectonic setting of Cretaceous to Quaternary volcanism in northwestern Iran, *Journal of Geodynamics* 47:167-179.

Barton M, Varekamp JC, Van Bergen MJ (1982) Complex zoning of clinopyroxenes in the lavas of Vulsini, Latium, Italy: evidence for magma mixing, *Journal of Volcanology and Geothermal Research* 14:361-388.

Bence A, Papike J, Ayuso R (1975) Petrology of submarine basalts from the Central Caribbean: DSDP Leg 15, *Journal of Geophysical Research* 80:4775-4804.

Bindi L, Cellai D, Melluso L, Conticelli S, Morra V, Menchetti S (1999) Crystal chemistry of clinopyroxene from alkaline undersaturated rocks of the Monte Vulture Volcano, Italy, *Lithos* 46:259-274

Bizimis M, Salters VJ, Bonatti E (2000) Trace and REE content of clinopyroxenes from supra-subduction zone peridotites. Implications for melting and enrichment processes in island arcs, *Chemical Geology* 165:67-85.

Brooks CK, Rucklidge JC (1973) A Tertiary lamprophyre dike with high pressure xenoliths and megacrysts from Wiedemanns Fjord, East Greenland, *Contributions to Mineralogy and Petrology* 42:197-212.

Canil D, Fedortchouk Y (2000) Clinopyroxene-liquid partitioning for vanadium and the oxygen fugacity during formation of cratonic and oceanic mantle lithosphere, *Journal of Geophysical Research* 105:246.

Dal Negro A, Carbonin S, Molin G, Cundari A, Piccirillo E (1982) Intracrystalline cation distribution in natural clinopyroxenes of tholeiitic, transitional, and alkaline basaltic rocks. In: Advances in physical geochemistry. Springer, pp 117-150.

Dal Negro A, Cundari A, Piccirillo E, Molin G, Uliana D (1986) Distinctive crystal chemistry and site configuration of the clinopyroxene from alkali basaltic rocks, *Contributions to Mineralogy and Petrology* 92:35-43.

Dal Negro A, Manoli S, Secco L, Piccirillo EM (1989) Megacrystic clinopyroxenes from Victoria (Australia): crystal chemical comparisons of pyroxenes from high and low pressure regimes, *European Journal of Mineralogy*:105-122.

Dawson J (1987) Metasomatized harzburgites in kimberlite and alkaline magmas: enriched restites and "flushed" lherzolites, *Mantle Metasomatism*:125-144

Dobosi G, Fodor R (1992) Magma fractionation, replenishment, and mixing as inferred from green-core clinopyroxenes in Pliocene basanite, southern Slovakia, *Lithos* 28:133-150.

Dobosi G, Horváth I (1988) High-and low-pressure cognate clinopyroxenes from alkali lamprophyres of the Velence and Buda Mountains, Hungary, *N Jb Mineral Abh* 158:241-256.

Duda A, Schmincke H-U (1985) Polybaric differentiation of alkali basaltic magmas: evidence from green-core clinopyroxenes (Eifel, FRG), *Contributions to Mineralogy and Petrology* 91:340-353.

Federico M, Gianfagna A, Aurisicchio C (1988) Clinopyroxene chemistry of the high-potassium suite from the Alban Hills, Italy, *Mineralogy and Petrology* 39:1-19.

Ghorbani MR, Middlemost EA (2000) Geochemistry of pyroxene inclusions from the Warrumbungle Volcano, New South Wales, Australia, *American Mineralogist* 85:1349-1367.

Hamilton D, Burnham CW, Osborn E (1964) The solubility of water and effects of oxygen fugacity and water content on crystallization in mafic magmas, *Journal of Petrology* 5:21-39.

Jamali H, Yaghubpur A, Mehrabi B, Dilek Y, Daliran F, Meshkani A (2012) Petrogenesis and Tectono-Magmatic Setting of Meso-Cenozoic Magmatism in Azerbaijan Province, Northwestern Iran. Petrology – New Perspectives and Applications. InTech China.

Malgarotto C, Molin G, Zanazzi PF (1993) Crystal chemistry of clinopyroxenes from Filicudi and Salina (Aeolian Islands, Italy). Geothermometry and barometry, *European journal of mineralogy* 5:915-923.

Manoli S, Molin G (1988) Crystallographic procedures in the study of experimental rocks: X-ray single-crystal structure refinement of C2/c clinopyroxene from Lunar 74275 high-pressure experimental basalt, *Mineralogy and petrology* 39:187-200.

Moayyed M (2001) Investigation of Tertiary volcano-plutonic bodies in west Alborz-Azarbayejan (Hashtjin area). PhD Thesis, Shahid Beheshti University, Iran, (in Persian).

Morimoto N, Ferguson A, Ginzburg I, Ross M, Seifert F, Zussman J, Aoki A, Gottardi G (1988) Nomenclature of Pyroxenes, *American Mineralogist* 1:131-145.

Nazzareni S, Molin G, Peccerillo A, Zanazzi P (2001) Volcanological implications of crystal-chemical variations in clinopyroxenes from the Aeolian Arc, Southern Tyrrhenian Sea (Italy), *Bulletin of Volcanology* 63:73-82.

Nimis P (1995) A clinopyroxene geobarometer for basaltic systems based on crystal-structure modeling, *Contributions to Mineralogy and Petrology* 121:115-125.

Nimis P (1999) Clinopyroxene geobarometry of magmatic rocks. Part 2. Structural geobarometers for basic to acid, tholeiitic and mildly alkaline magmatic systems, *Contributions to Mineralogy and Petrology* 135:62-74.

Nimis P, Ulmer P (1998) Clinopyroxene geobarometry of magmatic rocks Part 1: An expanded structural geobarometer for anhydrous and hydrous, basic and ultrabasic systems, *Contributions to Mineralogy and Petrology* 133:122-135.

Papike J, Cameron K, Baldwin K Amphiboles and pyroxenes: characterization of other than quadrilateral components and estimates of ferric iron from microprobe data. In: Geological Society of America, Abstracts with Programs, 1974. pp 1053-1054.

Perugini D, Busa T, Poli G, Nazzareni S (2003) The role of chaotic dynamics and flow fields in the development of disequilibrium textures in volcanic rocks, *Journal of Petrology* 44:733-756

Perugini D, Poli G, Gatta G (2002) Analysis and simulation of magma mixing processes in 3D, *Lithos* 65:313-330.

Princivalle F, Tirone M, Comin-Chiaramonti P (2000) Clinopyroxenes from metasomatized spinel-peridotite mantle xenoliths from Nemby (Paraguay): crystal chemistry and petrological implications, *Mineralogy and Petrology* 70:25-35.

Putirka K, Ryerson F, Mikaelian H (2003) New igneous thermobarometers for mafic and evolved lava compositions, based on clinopyroxene+ liquid equilibria, *American Mineralogist* 88:1542-1554.

Sazonova L, Nosova A (1999) Clinopyroxene zoning as an Indicator of the magmatic melt cooling conditions: an example of odinites from the Urals, *Geochemistry International* 37:1141-1157.

Shaw CS, Eyzaguirre J (2000) Origin of megacrysts in the mafic alkaline lavas of the West Eifel volcanic field, Germany, *Lithos* 50:75-95.

Shimizu N (1990) The oscillatory trace element zoning of augite phenocrysts, *Earth-Science Reviews* 29:27-37.

Simonetti A, Shore M, Bell K (1996) Diopside phenocrysts from nephelinite lavas, Napak Volcano, eastern Uganda; evidence for magma mixing, *The Canadian Mineralogist* 34:411-421.

Vollmer R, Johnston K, Ghiara M, Lirer L, Munno R (1981) Sr isotope geochemistry of megacrysts from continental rift and converging plate margin alkaline volcanism in south Italy, *Journal of Volcanology and Geothermal Research* 11:317-327.

Wass SY (1979) Multiple origins of clinopyroxenes in alkali basaltic rocks, *Lithos* 12:115-132.

Zhu Y, Ogasawara Y (2004) Clinopyroxene phenocrysts (with green salite cores) in trachybasalts: implications for two magma chambers under the Kokchetav UHP massif, North Kazakhstan, *Journal of Asian Earth Sciences* 22:517-527 doi:10.1016/s1367-9120(03)00091-9.